International Journal of Scientific & Engineering Research Volume 14, Issue 1, January-2023 447
ISSN 2229-5518

Aerodynamic Optimization and Electrification of Auto-Rickshaws

Herambh Dakshinamoorthy

Abstract— Auto-rickshaws are among the most widely used public transportation means in most Asian cities, providing fast and inexpensive end-to-end connectivity. The rickshaws, however, contribute to large amounts of environmental pollution despite the introduction of compressed natural gas (CNG) and liquified petroleum gas (LPG) models. The poor aerodynamic design of the auto-rickshaws lowers the vehicle's performance, making it highly energy-inefficient. However, very few studies have explored how the design can be made more aerodynamically efficient. By switching from an internal combustion engine to an electric vehicle powertrain, auto-rickshaws can be made more energy efficient and environmentally sustainable as they produce no emissions. This work aims to identify the shortcomings of the existing design and ways in which it can be improved. An in-depth analysis of the existing auto-rickshaw is carried out, and the drag force is calculated from the computational fluid dynamics (CFD) simulations on SimScale CFD. Possible design shortcomings are listed from aerodynamic principles and validated using the results obtained from the simulations. An optimized design is made using SOLIDWORKS to overcome these shortcomings, and it is validated on SimScale CFD. Electric vehicle powertrain calculations are then performed for this improved design using MATLAB and Simulink. This paper provides new insights into an aerodynamically-optimized design of an electric rickshaw to improve the energy-efficiency to provide environmentally sustainable transportation.

Index Terms— Auto-Rickshaw, Aerodynamic Optimization, Electric Powertrain, Environmentally Sustainable Transportation, Energy-Efficiency

1 INTRODUCTION

With the rising global pollution levels over the last decade, India ranks fifth on the list of countries with the worst air quality and pollution in the world [1]. Vehicular emissions have been a major contributor to this falling air quality and rising air pollution in India. Three-wheeled auto rickshaws are among the most widely used public transportation mediums in most Asian cities, including India. The conventional internal combustion engines used in these rickshaws generate emissions with high concentrations of particulate matter (PM), carbon dioxide (CO2), sulphur oxides (SOx), nitrogen oxides (NOx), and hydrocarbons (HC), which degrade the quality of the air and cause environmental pollution. In addition to their environmental impacts, IC engine auto rickshaws are highly energy-inefficient. They typically have a low fuel efficiency, which means they consume more fuel and emit more emissions per kilometer travelled compared to other vehicles. Also, a study by H.T. Anil and S. Arunima reveals that hearing loss was prevalent in approximately 40% of auto-rickshaw drivers [2]. Conventional auto-rickshaws with tampered silencers can produce up to 140 dB of noise.

Over the last decade, the auto-rickshaw market has seen a rise in liquified petroleum gas (LPG) and compressed natural gas (CNG) models to mitigate the pollution problem posed by conventional petrol and diesel models. Despite this, approximately 1200 tonnes of carbon dioxide and 4 tonnes of NOx, and 0.5 tonnes of PM10 are emitted from auto-rickshaws in Bangalore per day, according to a study conducted by The Energy Research Institute (TERI) [3].

Although electric rickshaws have been introduced in many cities over the past few years, the lack of a regulatory framework and the need to make inexpensive rickshaws has led to the downfall of product quality, performance, and safety. Therefore, the need arises to work on better designs compliant with the rules laid down by the Automotive Research Association of India (ARAI) to make safer, better performing, and more energy-efficient electric rickshaws.

This study aims to establish an aerodynamically optimized design for an electric auto-rickshaw after analyzing the shortcomings in the design and performance of conventional auto-rickshaws. The open-compartment design of the auto-rickshaws increases the aerodynamic drag experienced by the vehicle and also increases fuel consumption and emissions. These rickshaws can be made more energy-efficient by optimizing their design based on aerodynamic principles. By optimizing the rickshaw's drag coefficient, we can achieve lower consumption, cutting down on the weight and cost of the electric powertrain while making it more environmentally sustainable.

A 30% switch from conventional three-wheelers to electric three-wheelers by 2030 would result in a 20% reduction in energy consumption and a 7% reduction in CO2 emissions. Furthermore, switching to electric power for all three-wheelers on the road by 2050 would result in a 75% reduction in energy use and an 18% reduction in CO2 emissions compared to business as usual [4].

Electric rickshaws produce minimal amounts of emissions as compared to their internal combustion engine counterparts. Because they have fewer moving parts than combustion engine vehicles, they are more efficient and easier to maintain. Furthermore, using renewable energy sources to produce electricity to power these rickshaws would allow them to function as zero-emission vehicles and eliminate the possibility of indirect air pollution. Fewer moving parts also eliminate a huge issue in conventional auto-rickshaws — noise pollution. Electric rickshaws operate quietly and produce significantly lesser noise.

2 Baseline Rickshaw

2.1 Baseline Auto-Rickshaw Design

India's largest three-wheeler OEM, Bajaj Auto, had a market share of 50.6% in the fiscal year 2021 [5]. One of the most common combustion engine auto rickshaws currently being used is the Bajaj RE Compact 4S LPG. The specifications of this are shown in Table 1 [6].

TABLE 1
Bajaj RE Compact 4S LPG Specifications

Specification	Value
Length (mm)	2635
Width (mm)	1300
Height (mm)	1704
Wheelbase (mm)	2000
Vehicle Kerb Weight (kg)	368
Maximum Gross Vehicle Weight (kg)	698
Maximum Net Power (kW at 6000 rpm)	8.4
Maximum Net Torque (Nm at 4250 rpm)	15.2
Seating	3+1
Top Speed (kmph)	52
Gear System	4 forward + 1 reverse
Gradeability	20%

The conventional auto rickshaw is a three-wheeled vehicle in the delta configuration. They are available in petrol, LPG, and CNG variants. Most models have space to accommodate three passengers in the rear, apart from the driver seated in the front. Doors are foregone, and the sides are left uncovered in the conventional rickshaw design to facilitate easy pick-up and drop-off and reduce the overall cost. However, this comes at the expense of passenger safety and comfort. A short wheelbase and trackwidth allow for easy maneuverability. Most three-seater models have a kerb weight in the range of 368 kg with a load-carrying capacity of 330 kg. The engine provides 8.4 kW of power and 15.2 N-m torque to provide the required acceleration and maximum speed. The four-gear speed system helps the auto-rickshaw provide quick pick-up and drop-off facilities with a top speed of 52 kmph.

The model is claimed to have a mileage of 40 kmpl [6], but this figure decreases drastically with continuous use. According to reports, the average distance travelled daily is around 100 km [8]. Therefore, the daily fuel consumption can be estimated to be around 2.5 L.

The energy consumption of the petrol variant can be calculated using the energy content of the petrol. Petrol produces about 32 MJ of energy per liter. Therefore, $2.5\,L \times 32\,MJ/L = 80\,MJ\ or\ 22.22\,kWh$ of energy is required per day to travel 100 km [9]. Similarly, the energy consumption of the diesel variant can be calculated using the energy content of diesel. Diesel produces approximately 36 MJ of energy per liter. Thus, $2.5\,L \times 36\,MJ/L = 90\,MJ\ or\ 25\,kWh$ of energy is required per day [9].

Energy and fuel consumption can be reduced along with emissions by reducing the force required to provide traction. Equations 1 and 2 show that the traction force is a sum of the acceleration, drag, rolling resistance, and gradient forces. Since all the other forces are subject to constraints, the aerodynamic drag force is the only term we can minimize. The drag force on the auto-rickshaw can be minimized by minimizing the drag coefficient c_d and the frontal area A.

$$F = F_a + F_d + F_{rr} + F_\theta \quad (1)$$

$$F = ma + \frac{1}{2}\rho c_d A\, v^2 + \mu_{rr} mg\cos\theta + mg\sin\theta \quad (2)$$

By identifying the key drawbacks in the aerodynamics of the existing auto rickshaw design, we can design a new aerodynamically optimized auto rickshaw. To identify potential problems in the current design, the Bajaj RE Compact 4S model was created on the 3-D modelling software SOLIDWORKS 2022 using the original design drawings. The model was then exported as a Parasolid file and used for computational fluid dynamics (CFD) analysis.

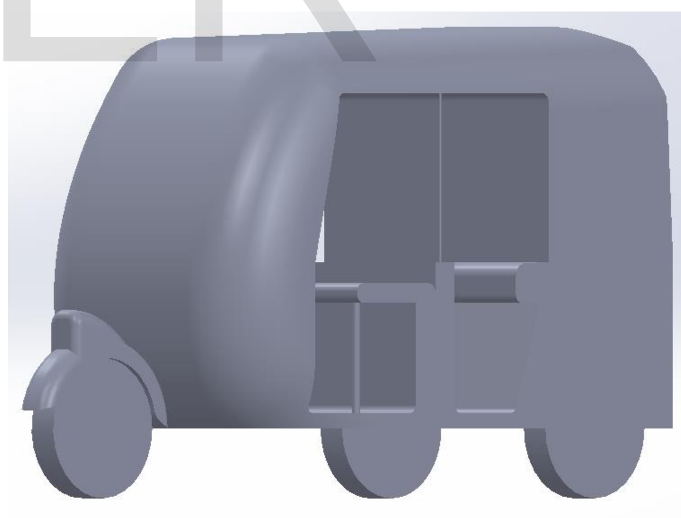

(a)

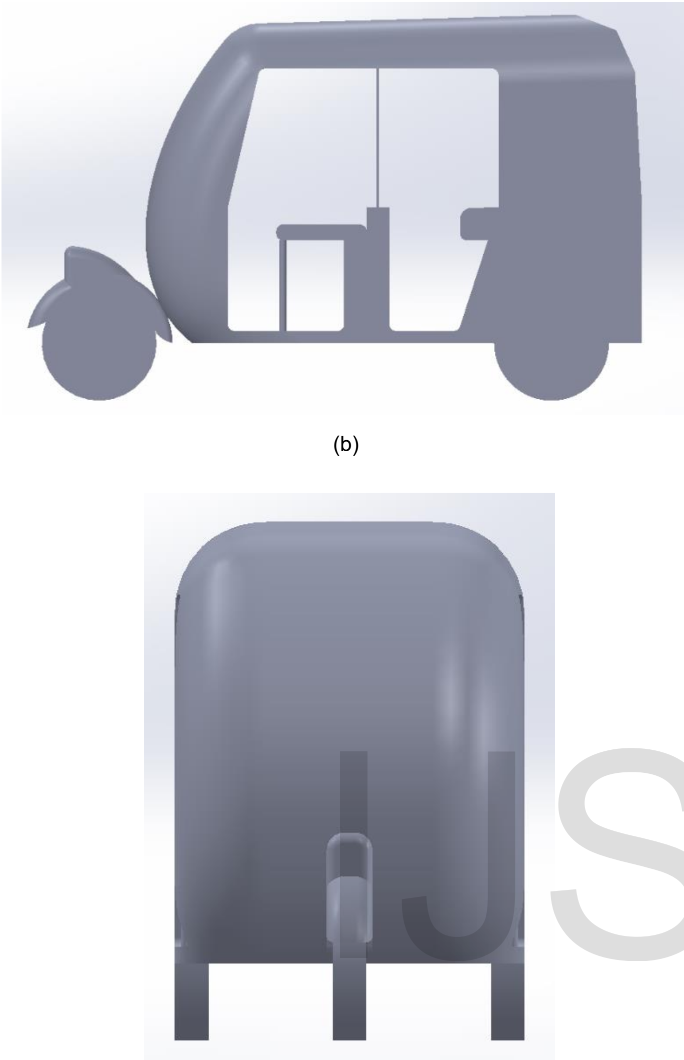

(b)

(c)

Fig. 1 – Baseline Rickshaw Design

2.2 Analysis of the Baseline Auto-Rickshaw Design

The aerodynamic drag force results from the pressure and the shear stress distribution. The drag experienced due to the pressure distribution is known as pressure drag (or form drag), and the drag experienced due to the shear stress distribution on the surface of the solid object is known as the skin friction drag. The pressure drag depends on how the fluid flows around the solid object, whereas the skin friction drag depends on the coefficient of viscosity of the fluid and its velocity gradient. In automobiles, the pressure drag contributes more significantly than the skin friction drag since all vehicles are bluff bodies [10]. In order to minimize the pressure difference generated due to the vehicle's body disrupting the flow of air around it, the vehicle's shape can be modified to allow the air to flow smoothly around it and delay the flow separation. The flow separation is caused due to an adverse pressure gradient along the body surface. This separation results in the formation of a low-pressure zone, leading to the formation of wakes. A resultant force then acts from the region of high pressure to the low-pressure region, causing a drag on the vehicle.

The computational fluid dynamics simulation was carried out using SimScale CFD, a cloud-based simulation software, to determine the original auto-rickshaw design's drag force and drag coefficient. The model's symmetry was used to our advantage to reduce computational time and memory. The geometry was then enclosed in a fluid flow region with the dimensions mentioned in Table 2, and a water-tight geometry was created. The fluid region was extended to three vehicle lengths behind the auto rickshaw to capture the wake flow characteristics accurately.

TABLE 2
SPECIFICATIONS OF FLUID FLOW REGION

Direction	Value
X min	0
X max	2.7 m
Y min	-0.3 m
Y max	2.7 m
Z min	-4.05 m
Z max	9.45 m

A body of influence was created in the form of a Cartesian box close to the auto-rickshaw body, as shown in Figure 2, to capture the vortices more accurately with the help of a finer mesh of 0.02 m maximum edge length. The local element size on the faces of the auto rickshaw was set to a maximum edge length of 0.005 m. The mesh was then resolved to accurately capture the geometric features of interest in the model and the areas with essential velocity and pressure gradients, as shown in Figure 3.

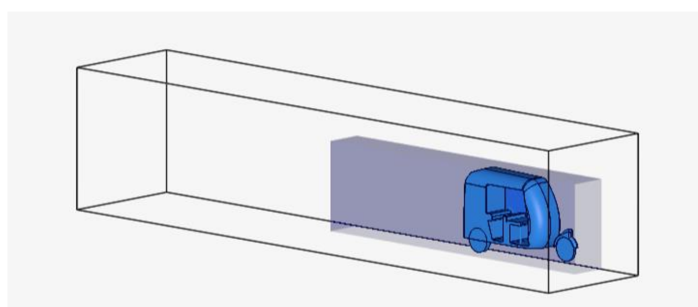

Fig. 2 – Cartesian Box with Fluid Flow Region

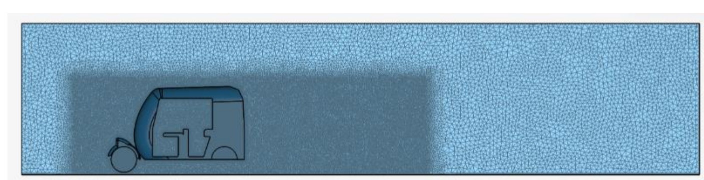

Fig. 3 – Mesh of the Baseline Environment

ISSN 2229-5518

The material properties were set once this was done. Air was chosen as the material for the fluid flow region with a kinematic viscosity (υ) of 1.529e-5 m^2/s and a density (ρ) of 1.196 kg/m^3. The SST k-ω physical model was chosen to model turbulent flow, and the boundary conditions were prescribed at all the boundary zones. The initial and boundary conditions are shown in Table 3 and Table 4, respectively. The last step was to set up the solver controls. Once this was done, the simulation was run.

TABLE 3
INITIAL CONDITIONS

Properties	Value
Pressure	0 Pa
Velocity	0 m/s
Turbulent Kinetic Energy Value	0.00375 m^2/ s^2
Specific Turbulence Dissipation Rate	3.375 1/s

TABLE 4
BOUNDARY CONDITIONS

Properties	Value
Velocity Inlet	8.33 m/s (30 kmph)
Pressure Outlet	0 Pa
Symmetry	1 Face
Wall	2 Walls with Slip + 1 Moving Wall

2.3 Results

The simulation results were examined, and the post-processing results were visualized using pressure and velocity plots. Figure 4 shows the plot of pressure drag force and viscous (or friction) drag force versus simulation iterations. The pressure drag force experienced on one symmetry half is 14.32 N, and the viscous drag force is 0.75 N. Therefore, the total drag force acting on the auto-rickshaw is 30.15 N at 30 kmph. Figure 5 shows the plot of the drag coefficient versus simulation iterations. The drag coefficient is approximately 0.36. Figures 6 and 7 show the surface plots of pressure and velocity, respectively.

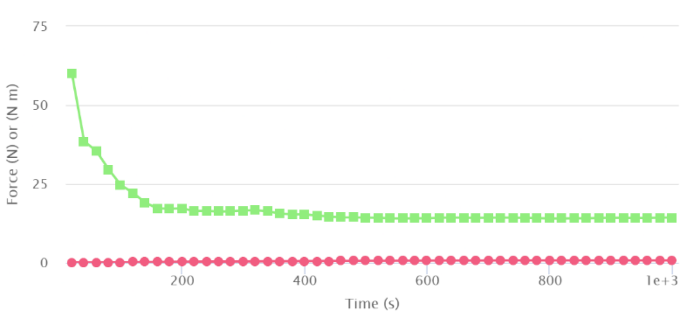

Fig. 4 – Drag Force on Baseline Rickshaw

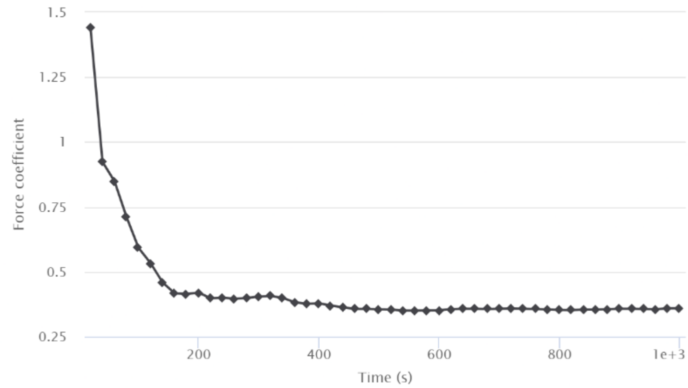

Fig. 5 – Drag Coefficient of Baseline Rickshaw

Fig. 6 – Pressure Surface Plot of Baseline Rickshaw

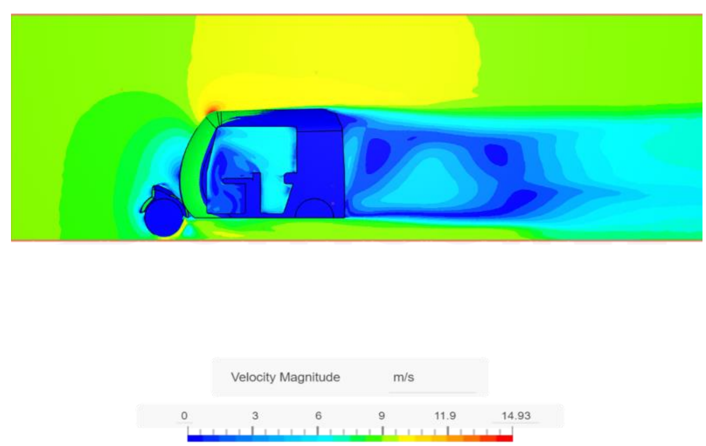

Fig. 7 – Velocity Surface Plot of Baseline Rickshaw

2.4 Discussion

In order to reduce the amount of energy consumption and emissions associated with the conventional IC engine auto rickshaw, the aerodynamic resistance experienced by it must be minimized. With a drag coefficient of 0.36 and a total drag force of 30.15 N, the current auto rickshaw design would consume about 3014.60 kJ/day (assuming the rickshaw travels 100 km/day) due to the aerodynamic drag. In order to minimize the drag force and the drag coefficient, the pressure and velocity plots need to be analyzed, and appropriate modifications must be made in the new design.

It can be seen from the surface pressure plot that there is a high-pressure concentration at the front wheel and the front of the auto-rickshaw. This pressure drops drastically on moving along the length of the vehicle. The frontal area of the auto-rickshaw has minimal curvature making it difficult for the air to flow around this section. This causes a high drag resistance due to the pressure developed in that region. Adding more curvature to the frontal area would help the airflow around the front more easily. The open compartment design (absence of doors) causes the flow separation in the sides to occur very soon. This allows the air to flow into the interior of the auto-rickshaw, which causes an additional drag force on the inside of the auto-rickshaw. Thus, the open compartment design significantly contributes to the vehicle's aerodynamic drag. With proper usage of doors on the sides, this flaw can be eliminated while providing more safety to the drivers. The roof has a slight upward slope from the front to the rear, followed by a sharp turn to the rickshaw's base region (rearmost region). This causes the flow to separate, resulting in the formation of a low-pressure region behind the rickshaw. A downward slope from the front to the rear can help delay flow separation.

3 Optimized Rickshaw

3.1 Optimized Auto-Rickshaw Design

An aerodynamically optimized auto rickshaw would help reduce energy consumption and emissions by a substantial margin. However, it should be kept in mind to keep the essential parameters of the auto-rickshaw unaltered so that its basic functionality and vehicle dynamics are not affected. Thus, the new auto rickshaw is designed with a similar wheelbase, trackwidth and dimensions. The driver and passenger comfort and ergonomics should not be affected as well.

In order to minimize the drag on the auto-rickshaw, many changes were made to the overall envelope of the rickshaw and a few modifications to the exterior. The curvature of the auto-rickshaw's frontal surface is increased to allow the air to flow around it more smoothly and decrease the pressure gradient in this region. The open compartment design is foregone and replaced with a closed envelope. This helps delay the flow separation and eliminates the extra drag produced due to the internal flow within the compartment. A downward slope is given to the roof of the rickshaw to delay the flow separation and reduce the drag. Drag reduction can be achieved through re-pressurization within the base region. This can be done by bleeding the air around the base region. Features are added to the rickshaw's exterior near the base and bottom to bleed air. The air was bled from high-pressure regions near the bottom and base of the rickshaw. The rear is also chamfered to allow air to flow around the vehicle easily.

The newly optimized design was also made using SOLIDWORKS 2022. Iterations of the design were made and then analyzed on SOLIDWORKS Flow Simulation to pick the best parameters to optimize the design. The frontal surface curvature, the angle of the slope on the roof, the fillet size, and the position of the air bleeding features were fine-tuned to provide the best possible results. A total of six iterations were performed to obtain the final optimized model. The specifications of the final iteration of the new design are listed in Table 5.

(a)

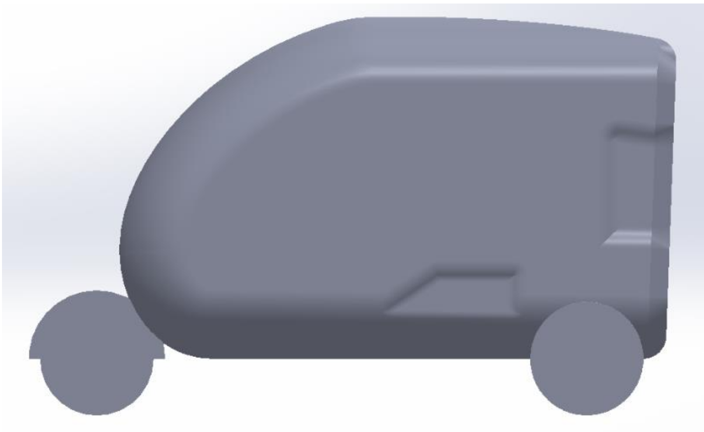

(b)

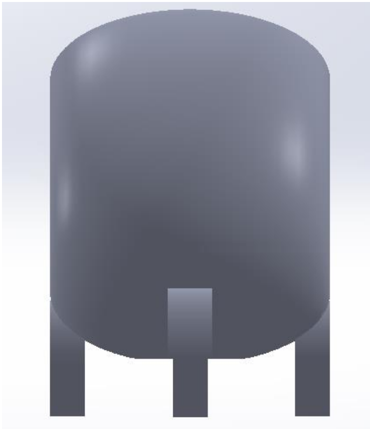

(c)
Fig. 8 – Optimized Auto-Rickshaw Design

TABLE 5
OPTIMIZED AUTO-RICKSHAW DESIGN SPECIFICATIONS

Specification	Value
Length (mm)	2830
Width (mm)	1200
Height (mm)	1623
Wheelbase (mm)	2100
Frontal Area (m^2)	1.9
Seating	3+1

3.2 Analysis of Optimized Auto-Rickshaw Design

The new design is then simulated on SimScale CFD using a process similar to that followed for the analysis of the baseline rickshaw design. The dimensions of the fluid flow region are mentioned in Table 6.

A Cartesian box was created around the auto-rickshaw body with a maximum edge length of 0.02 m. The local element size on the faces of the auto rickshaw was set to a maximum edge length of 0.005 m.

The same material properties were set as described in the analysis of the baseline auto-rickshaw model. The SST k-ω physical model was used, and the initial and boundary conditions are shown in Table 3 and Table 4, respectively. The last step was to set up the solver controls. Once this was done, the simulation was run.

TABLE 6
SPECIFICATIONS OF FLUID FLOW REGION

Direction	Value
X min	0
X max	2.83 m
Y min	-1.3 m
Y max	2.83 m
Z min	-14.15 m
Z max	4.19 m

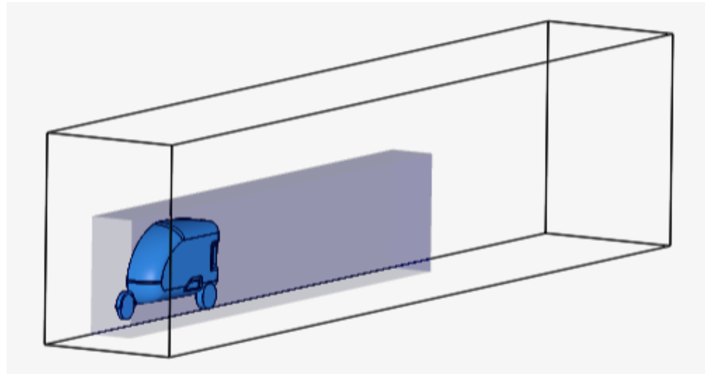

Fig. 9 – Cartesian Box with Fluid Flow Region

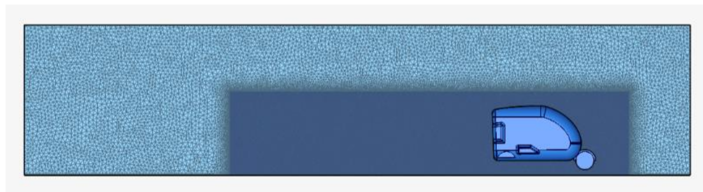

Fig. 10 – Mesh of Optimized Model

3.3 Results

The plot of pressure drag force and viscous drag force versus simulation iterations is shown in Figure 11. The negative sign arises due to the orientation of the forces along the negative z-direction. The pressure drag force acting on one symmetry half is 11.55 N, and the viscous drag force is 0.88 N. Hence, the total drag force acting on the auto-rickshaw is 24.85 N at 30 kmph. Figure 12 shows the plot of the drag coefficient versus simulation iterations. The coefficient of drag is approximately 0.31. Figures 13 and 14 show the surface plots of pressure and velocity, respectively.

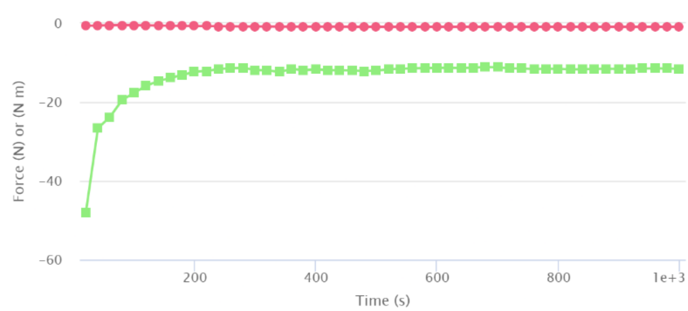

Fig. 11 – Drag Force on Optimized Rickshaw

3.4 Discussion

The results show a significant reduction in the drag force and the drag coefficient of the auto-rickshaw. The optimized design has a drag coefficient as low as 0.31 and a drag force of 24.85 N at a speed of 30 kmph. This means that there would also be a corresponding reduction in the amount of traction force and the vehicle's power consumption. The energy consumption per day (assuming the rickshaw travels 100 km/day) due to aerodynamic drag reduces to 2485.42 kJ.

It can be seen that this design has appreciably lower energy consumption than the current auto rickshaw design, consuming 529.18 kJ lesser energy per day. This is a result of the reduction in the drag coefficient that we have achieved as a result of the modifications in the design. The new design has a drag coefficient of 0.31, a reduction of 0.05.

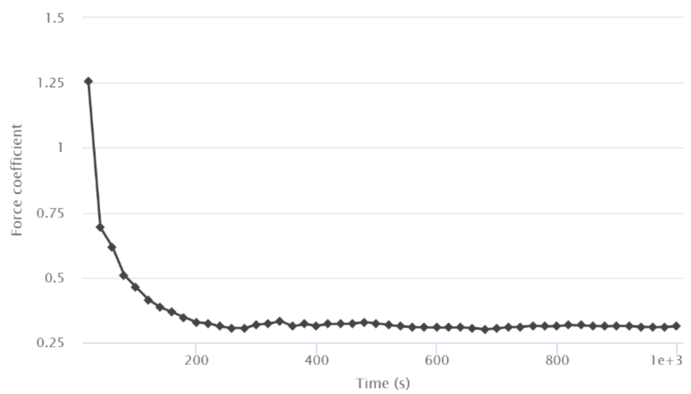

Fig. 12 – Drag Coefficient of Optimized Rickshaw

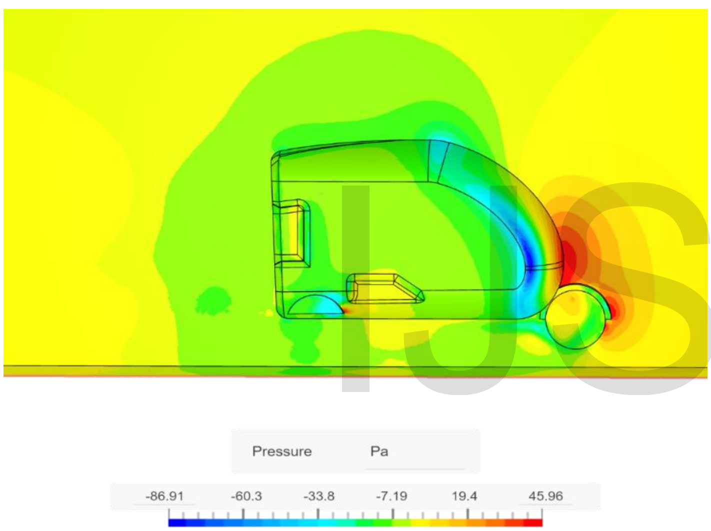

Fig. 13 – Pressure Surface Plot of Optimized Rickshaw

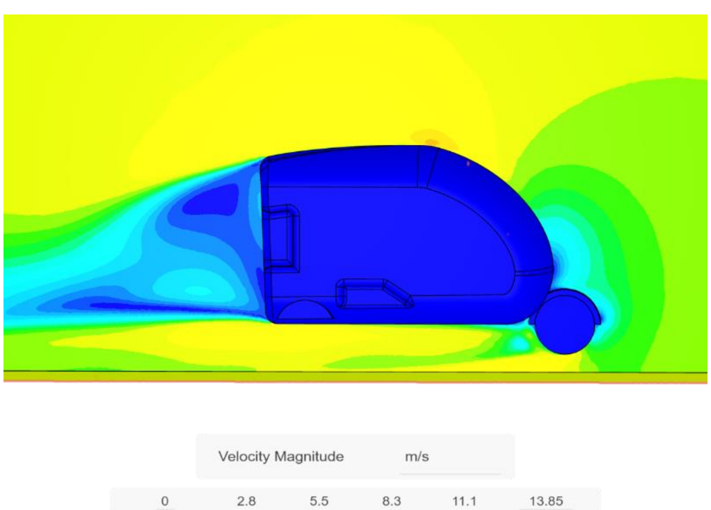

Fig. 14 – Pressure Surface Plot of Optimized Rickshaw

4 Electric Powertrain

One possible way to further improve the energy efficiency of the auto-rickshaw design is to consider switching to an electric vehicle (EV) powertrain. EVs are propelled by electric motors rather than internal combustion engines, meaning they do not produce emissions or require fossil fuels. An EV powertrain can also be more efficient than an internal combustion engine, as it does not waste energy through combustion and can recover energy through regenerative braking. Shifting to an electric vehicle powertrain would contribute zero harmful emissions making it a highly-sustainable and environment-friendly transportation mode.

To find the motor power and torque requirements, we first calculate the total traction force required to provide the required acceleration and top speed. The traction force required can be calculated using Equation 3.

$$F = ma + \frac{1}{2}\rho c_d A\, v^2 + \mu_{rr} mg\cos\theta + mg\sin\theta \qquad (1)$$

The traction force F can also be written as a function of the gear ratio, the motor torque, and the wheel's radius.

$$F = \frac{GT}{r} \qquad (2)$$

Equating Equations 3 and 4, we get,

$$\frac{GT}{r} = ma + \frac{1}{2}\rho c_d A\, v^2 + \mu_{rr} mg\cos\theta + mg\sin\theta \qquad (3)$$

Upon simplifying and rearranging, we get,

$$v_{n+1} = v_n + \left(\frac{GT}{mr} - \frac{1}{2m}\rho c_d A\, v_n^2 - \mu_{rr} g\cos\theta - g\sin\theta\right)\Delta t \qquad (4)$$

With the help of these equations, a Simulink model is made to perform the motor simulation, as shown in Figure 16. The specifications of the rickshaw are as mentioned in Table 7. The Modified Indian Driving Cycle (MIDC) was adopted for vehicle certification for emissions and safety. Its equivalent, the New European Driving Cycle (NEDC), is used for this simulation. The first 800 seconds (Part 1) of this cycle are used for our simulation as the top speed of auto rickshaws in India is only around 50 kmph. The velocity and acceleration plots of the NEDC are shown in Figure 15.

We can see that the power requirement has a torque requirement to provide similar top speeds and accelerations. The target acceleration is 1 m/s^2 and the target velocity is 50 kmph. The values of peak power, peak torque, and gear ratio are varied in order to help achieve the targets. For the motor simulation, the time step is set to 0.01 s, and the simulation time is set to 20 s. The plots of velocity, acceleration, power and torque are shown in Figures 17-20. The specifications of the motor are shown in Table 8.

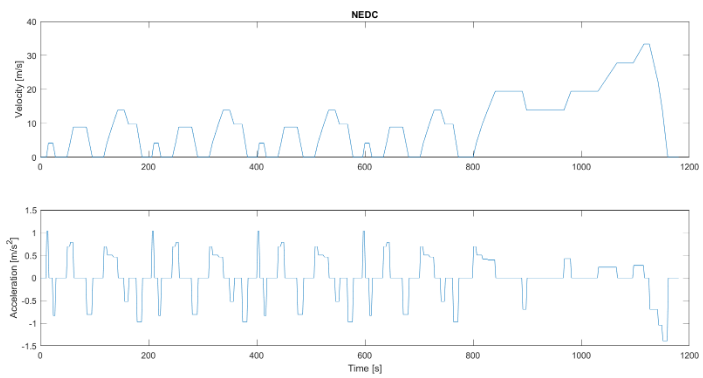

Fig. 15 – New European Drive Cycle

TABLE 7
SPECIFICATIONS OF OPTIMIZED AUTO-RICKSHAW

Parameter	Value
Kerb Weight	450 kg
Gross Vehicle Weight	750 kg
Rolling Resistance	0.02
Coefficient of Drag (C_d)	0.31
Range to be provided	120 km
Frontal Area	1.9 m^2

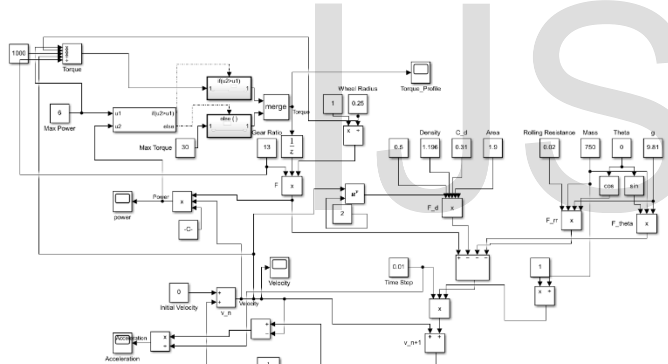

Fig. 16 – Motor Simulink Model

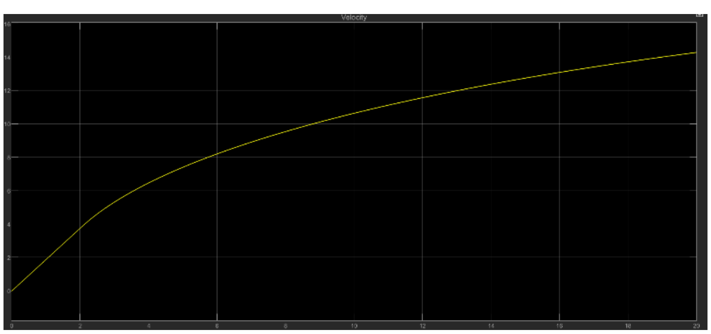

Fig. 17 – Velocity vs Time Plot

In order to calculate the specifications of the battery pack, the energy requirement of the rickshaw must be known. That can be found out using Equation 7.

$$Energy = \frac{Total\ Energy\ Required\ from\ Drive\ Cycle}{Sample\ Distance\ Used\ in\ Drive\ Cycle\ Calculation} \times Range \quad (7)$$

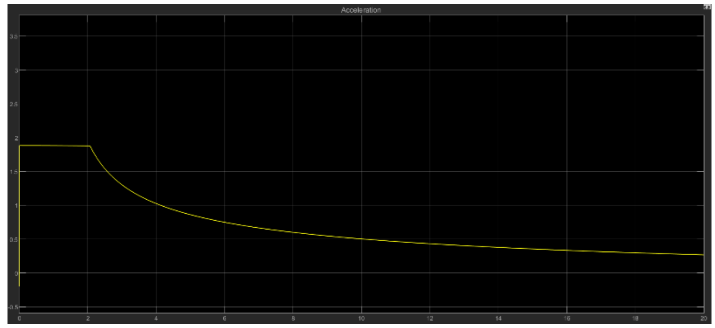

Fig. 18 – Acceleration vs Time Plot

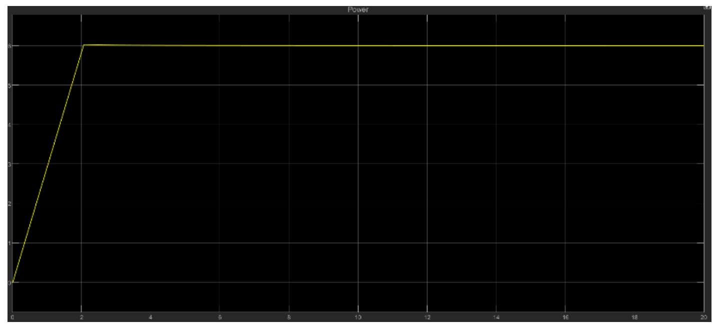

Fig. 19 – Power vs Time Plot

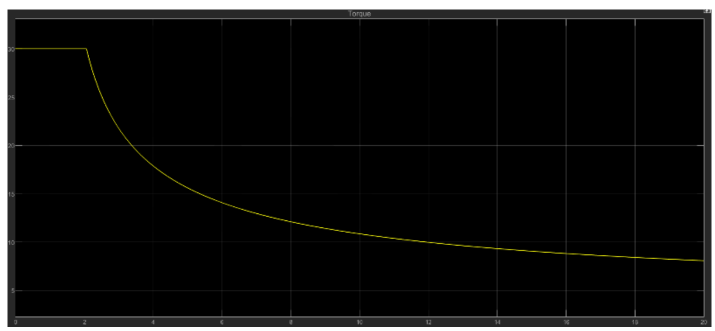

Fig. 20 – Torque vs Time Plot

The capacity of the battery pack can be found out using Equation 8.

$$Capacity = \frac{Energy}{Voltage} \quad (5)$$

The number of cells in series is given by the equation,

$$n = \frac{Total\ Voltage}{Individual\ Cell\ Voltage} \quad (6)$$

Similarly, the number of such strings in parallel is

$$m = \frac{Total\ Capacity}{Individual\ Cell\ Capacity} \quad (7)$$

Therefore, the total number of cells required is $n \times m$.

The model shown in Figure 21 uses the above-stated equations to perform battery pack sizing. The target range is set as 120 km. The battery pack voltage is set at 48 V as it provides an efficient power distribution while minimizing the losses involved in transmission. The individual cell voltage is 12 V, and the cell capacity is 40 Ah. The specifications of the battery pack

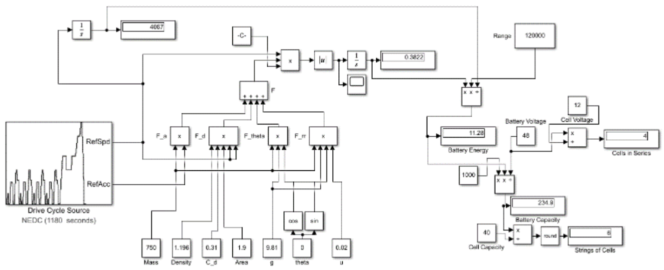

Fig. 21 – Battery Simulink Model

are shown in Table 8.

TABLE 8
SPECIFICATIONS OF ELECTRIC POWERTRAIN

Specification	Value
Motor Peak Torque	30 N-m
Motor Peak Power	6 kW
Gear Ratio	13
Battery Pack Voltage	48 V
Battery Pack Energy	11.52 kWh
Battery Pack Capacity	240 Ah
Battery Pack Configuration	12 V, 40 Ah cells in 4s 6p

5 CONCLUSION

Apart from being the most widely used public transportation form for passengers and goods in India for providing quick and inexpensive end-to-end connectivity, auto rickshaws hold the potential to promote green and sustainable transport. Auto-rickshaws promote an integrated public transport system, thereby stalling the growth of private car ownership and encouraging shared transport. In addition, on average, auto-rickshaws can transport the same number of people, using only one-third of the parking space and occupying half the space when travelling as a car [11].

The results of this study have important implications for the transportation industry and efforts to promote sustainable development. Auto rickshaws are a common mode of transportation in many developing countries, and improving their energy efficiency can significantly impact fuel consumption and emissions in these regions. By streamlining the body, optimizing the shape and size of the vehicle, and adding external features, we significantly reduced drag and improved the auto rickshaw's overall energy efficiency. In addition, we found that switching to an electric powertrain was another effective way to increase energy efficiency and reduce fuel consumption and emissions, making auto rickshaws one of the most environmentally friendly and sustainable transportation options.

REFERENCES

[1] IQAir, " 2021 World Air Quality Report," 2021.
[2] H. T. Anil and S. Arunima, "Noise Induced Hearing Loss in Autorickshaw Drivers in Bangalore: A Cross Sectional Study," p. 93–99, 2022.
[3] Palak Thakur and Sugandha Pal, "Estimating vehicular emissions from auto rickshaws plying in Bengaluru," *International Journal of Scientific,* p. 2241–2245, 2018.
[4] Chandan Bhavnani, Himanshu Shekhar and Arnesh Sharma TT, "Electric mobility paradigm shift: capturing the opportunities," TERI Council for Business Sustainability (CBS) & YES BANK, 2018.
[5] Shashank Kanodia and Jaimin Desai, "Bajaj Auto Ltd - Research and Analysis Report - ICICI Direct Research," ICICI Direct Research, 2021.
[6] Bajaj Auto, *Bajaj RE 4S Compact Brochure.*
[7] Bajaj Auto Finance, "Bajaj RE Petrol," [Online]. Available: https://www.bajajautofinance.com/three-wheeler-loan/Bajaj-RE-PETROL.
[8] Deepanjan Majumdar et al. "Study on possible economic and environmental impacts of electric vehicle infrastructure in public road transport in Kolkata," *Clean Technologies and Environmental Policy.*
[9] Putzig M. et al. "Fuel Properties Comparison Chart," U.S. Department of Energy, 2021.
[10] Gino Sovran, Thomas Morel and William T. Mason, Aerodynamic Drag Mechanisms of Bluff Bodies and Road Vehicles, Springer New York, NY, 1978.
[11] Akshay Mani, Madhav Pai and Rishi Aggarwal, "Sustainable Urban Transport in India: Role of the Auto-rickshaw Sector," 2012.
[12] James Larminie and John Lowry, Electric Vehicle Technology Explained, John Wiley and Sons, 2012.
[13] John Anderson, Fundamentals of Aerodynamics, McGraw Hill, 2017.